

## $R_K$ Measurement with NA62 at CERN SPS

---

**Giuseppe Ruggiero**<sup>\*†</sup>

CERN

E-mail: [giuseppe.ruggiero@cern.ch](mailto:giuseppe.ruggiero@cern.ch)

A precision measurement of the ratio  $R_K$  of the rates of kaon leptonic decays  $K^\pm \rightarrow e^\pm \nu$  and  $K^\pm \rightarrow \mu^\pm \nu$  with the full minimum bias data sample collected with low intensity 75 GeV/c beam by the NA62 experiment at CERN in 2007-2008 is reported. The result, obtained by analyzing about  $150 \times 10^3$  reconstructed  $K^\pm \rightarrow e^\pm \nu$  candidates with 11% background contamination, has a record precision of 0.4% and is in agreement with the Standard Model expectation.

*2013 Kaon Physics International Conference,  
29 April-1 May 2013  
University of Michigan, Ann Arbor, Michigan - USA*

---

<sup>\*</sup>Speaker.

<sup>†</sup>for the NA62 Collaboration.

## 1. Introduction

In the Standard Model (SM) the decays of charged pseudo scalar mesons into lepton neutrino ( $P^\pm \rightarrow l^\pm \nu$ , denoted  $P_{l2}$ ) are helicity suppressed. The SM allows a very precise determination of the ratio of  $P_{l2}$  decay amplitudes of the same meson in different lepton flavours, like  $R_K \equiv \Gamma(K_{e2})/\Gamma(K_{\mu2})$ . The prediction for  $R_K$  inclusive of internal bremsstrahlung (IB) radiation is [1]:

$$R_K^{SM} = \left(\frac{M_e}{M_\mu}\right)^2 \left(\frac{M_K^2 - M_e^2}{M_K^2 - M_\mu^2}\right)^2 (1 + \delta R_{QED}) = (2.477 \pm 0.001) \times 10^{-2}, \quad (1.1)$$

where  $\delta R_{QED}$  is an electromagnetic correction. Deviations of  $R_K$  from the SM require new physics models with sources of lepton flavour violation (LFV) [2, 3, 4]. Also  $R_K$  is sensitive to the neutrino mixing parameters within SM extensions involving a fourth generation of quarks and leptons [5] or sterile neutrinos [6].

The most precise measurements of  $R_K$  are from KLOE [7] and NA62 which analyzed a partial sample of the data set collected at CERN in 2007 [8]. They largely dominate the present PDG value [9] of  $R_K$ ,  $R_K = (2.488 \pm 0.012) \times 10^{-5}$ . A new measurement of  $R_K$  based on the full data sample collected by NA62 in 2007-08 is reported here [10].

## 2. Experimental Apparatus and Data Taking Conditions

The NA62 experiment at CERN collected data in 2007-08 for measuring  $R_K$  using the same beam line and experimental setup of the NA48/2 experiment [11]. The experiment made use of the 400 GeV/c primary proton beam, extracted from the SPS accelerator at CERN and producing a secondary charged kaon beam after impinging on a beryllium target. A 100 m long beam line selected the momentum of the secondary beam to  $(75 \pm 3)$  GeV/c. Finally the beam entered a decay volume, housed in a 100 m long vacuum tank. The detector was designed to see the products of the kaons decaying in the vacuum region. A magnetic spectrometer, consisted of four drift chambers separated by a dipole magnet, tracked the charged particles. It provided a transverse momentum kick of 265 MeV/c, corresponding to a momentum resolution of  $\sigma_p/p = (0.48 \oplus 0.009 \times p)\%$  ( $p$  in GeV/c). An array of scintillators (hodoscope) gave the time reference for the other detectors and the main trigger for the event topologies including charged particles. A quasi-homogeneous electromagnetic calorimeter with liquid Krypton as active material (LKr) [12] was used mainly for particle identification. The measured energy resolution is  $\sigma(E)/E = 0.032/\sqrt{(E)} \oplus 0.09/E \oplus 0.0042$  ( $E$  in GeV).

The trigger for  $K_{e2}$  decays made use of information from the hodoscope and the LKr in order to exploit the release of energy of the electron. About 65% of data were taken with the  $K^+$  beam only, 8% with the  $K^-$  only and the rest of time with simultaneous  $K^\pm$ . In order to measure directly on data the  $\mu$  - electron misidentification probability, 55% of data were collected with a lead bar in front of the LKr covering about 10% of the calorimetric acceptance. Four samples were analyzed independently, according to the sign of the kaon and to the presence or not of the lead bar ( $K^+(\text{noPb})$ ,  $K^+(\text{Pb})$ ,  $K^-(\text{noPb})$ ,  $K^-(\text{Pb})$ ).

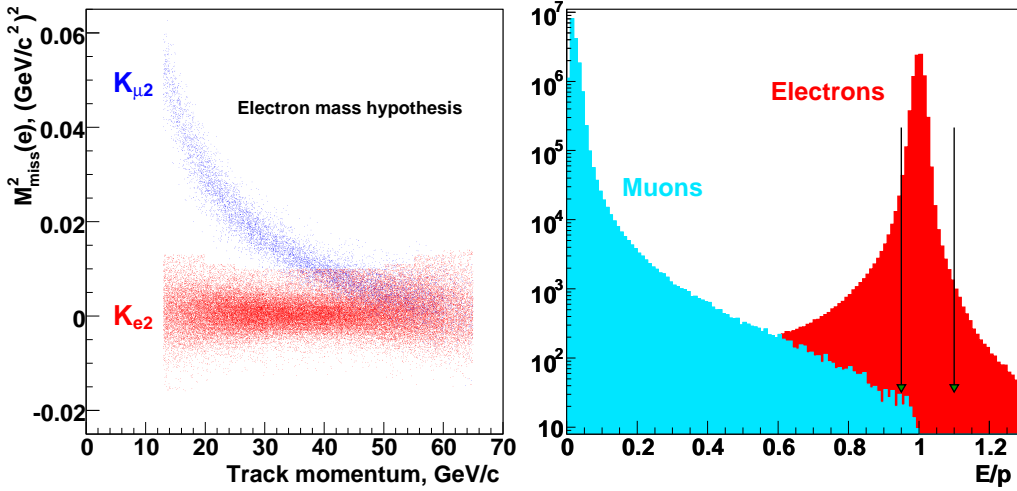


**Figure 1:** (left) Reconstructed squared missing mass in the electron mass hypothesis  $M^2_{\text{miss}}(e)$  as a function of lepton momentum for  $K_{e2}$  and  $K_{\mu 2}$  decays (data). (right)  $E/p$  spectra of electrons and muons (data) measured from  $K^\pm \rightarrow \pi^0 e^\pm \nu$  and  $K_{\mu 2}$  decays. The part of the muon spectrum above  $E/p = 0.95$  is for the muons traversing the Pb bar. The electron identification criterion applied for  $p > 25 \text{ GeV}/c$  is indicated with arrows.

### 3. Strategy of the Measurement

The analysis strategy for measuring  $R_K$  is based on counting the numbers of reconstructed  $K_{e2}$  and  $K_{\mu 2}$  events collected concurrently. Consequently  $R_K$  does not depend on the absolute kaon flux and the ratio allows for a first order cancellation of several systematic effects, like reconstruction and trigger efficiencies and time dependent biases. The basic formula is:

$$R_K = \frac{1}{D} \cdot \frac{N(K_{e2}) - N_B(K_{e2})}{N(K_{\mu 2}) - N_B(K_{\mu 2})} \cdot \frac{A(K_{\mu 2}) f_\mu \varepsilon(K_{\mu 2})}{A(K_{e2}) f_e \varepsilon(K_{e2})} \cdot \frac{1}{f_{LKr}}. \quad (3.1)$$

Here  $N(K_{l2})$  and  $N_B(K_{l2})$  are the number of selected  $K_{l2}$  events and expected background events, respectively;  $D$  is the downscaling factor applied to the  $K_{\mu 2}$  trigger;  $A(K_{l2})$  the geometrical acceptance of the selected  $K_{l2}$  mode;  $f_e$  and  $f_\mu$  the identification efficiencies of electrons and muons, respectively;  $\varepsilon(K_{l2})$  the trigger efficiencies for the selected  $K_{l2}$  events;  $f_{LKr}$  the global LKr efficiency. A Monte Carlo simulation is used to evaluate the acceptance correction and the geometric part of the acceptances for most of the background processes. The beam halo background, the particle identification and the readout and trigger efficiencies are measured directly from data. Both  $f_l$  and  $\varepsilon(K_{l2})$  are well above 99%. The analysis is performed independently for 40 data samples (10 bins of reconstructed lepton momentum and 4 different data samples).

### 4. Selection

Most of the selection criteria are common to both  $K_{e2}$  and  $K_{\mu 2}$  decay modes. These criteria identify events with a single-track topology and without clusters in the LKr not associated to the track via direct energy deposition or bremsstrahlung. The kinematics of the event and the lepton

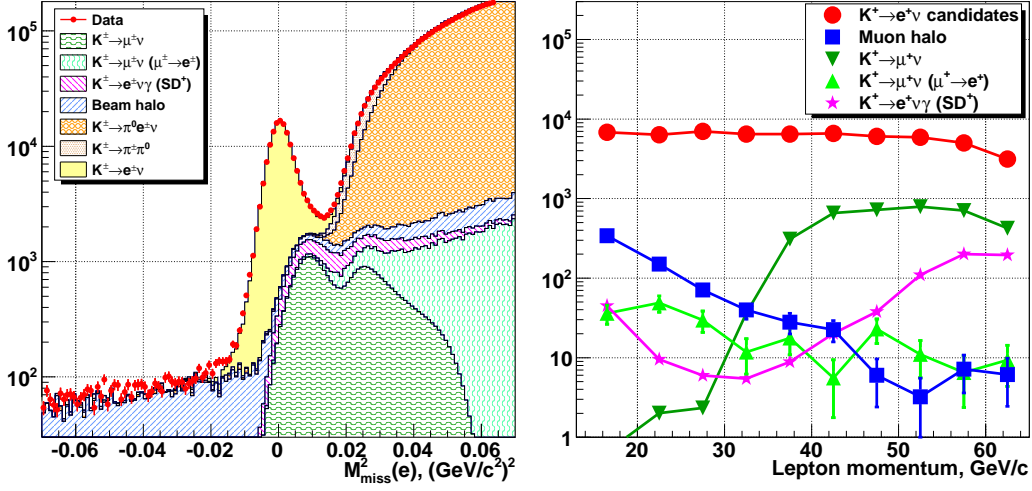


**Figure 2:** Distributions of reconstructed squared missing masses  $M_{miss}^2(e)$  for reconstructed  $K_{e2}$  events compared with the sums of normalized estimated signal and background components (left). Dependence of the background components in the  $K_{e2}$  sample on the measured lepton momentum for the data sample collected with  $K^+$  and no lead bar (right).

identification, instead, are effective to separate  $K_{e2}$  and  $K_{\mu 2}$ . The kinematic identification is based on the squared missing mass  $M_{miss}^2 = (P_K - P_l)^2$  (see figure 1 (left)), where  $P_K$  and  $P_l$  are the kaon and lepton 4-momenta respectively. The mean  $P_K$  is monitored on spill basis using fully reconstructed  $K^+ \rightarrow \pi^+ \pi^+ \pi^-$  decays;  $P_l$  is computed in the electron or muon mass hypothesis. A cut on the  $M_{miss}^2$ , according to the  $M_{miss}^2$  resolution and dependent on the lepton momentum, selects the  $K_{l2}$  candidates. The ratio between the energy deposited by the lepton in the calorimeter and the lepton momentum measured in the spectrometer ( $E/P$ ) allows the lepton identification (see figure 1 (right)). A cut on  $E/P$  between 0.95 (0.9 at  $P_l < 25 \text{ GeV}/c$ ) and 1.1 identifies the electrons; those tracks with  $E/P < 0.8$  are classified as muons.

## 5. Signal and Backgrounds

The total numbers of selected  $K_{e2}$  and  $K_{\mu 2}$  candidates are 145958 and  $4.2862 \times 10^7$ , respectively. Figure 2 (left) shows the distribution of the  $M_{miss}^2$  of reconstructed  $K_{e2}$  events with the backgrounds superimposed. Both data and a detailed simulation of the experiment allow a precise measurement of the background components. Table 1 reports the breakdown of the signal and backgrounds according to the 4 different data samples. Figure 2 (right) shows the background contamination in the  $K_{e2}$  sample as a function of the measured lepton momentum for the sample of positive kaons without the lead bar. The following sections describe the evaluation of the main backgrounds in the  $K_{e2}$  samples.

### 5.1 $K_{\mu 2}$ background in the $K_{e2}$ sample

The  $K_{\mu 2}$  background results mainly from muon misidentification due to hard bremsstrahlung in the LKr calorimeter. It has been addressed by a dedicated measurement of the misidentifica-

**Table 1:** Background contamination in the  $K_{\ell 2}$  samples integrated over lepton momentum. The uncertainties on the background in the  $K_{\mu 2}$  samples are negligible.

Data sample	$K^+$ (noPb)	$K^+$ (Pb)	$K^-$ (noPb)	$K^-$ (Pb)
$K_{e2}$ candidates	59813	63282	10530	12333
Muon halo	$(1.11 \pm 0.09)\%$	$(1.51 \pm 0.10)\%$	$(4.61 \pm 0.18)\%$	$(7.86 \pm 0.23)\%$
$K_{\mu 2}$	$(6.11 \pm 0.22)\%$	$(5.33 \pm 0.19)\%$	$(5.76 \pm 0.20)\%$	$(4.87 \pm 0.17)\%$
$K_{\mu 2}$ ( $\mu \rightarrow e$ decay)	$(0.26 \pm 0.04)\%$	$(0.27 \pm 0.04)\%$	$(0.31 \pm 0.09)\%$	$(0.19 \pm 0.07)\%$
$K^\pm \rightarrow e^\pm \nu \gamma$ (SD <sup>+</sup> )	$(1.07 \pm 0.05)\%$	$(4.01 \pm 0.18)\%$	$(1.25 \pm 0.06)\%$	$(3.95 \pm 0.17)\%$
$K^\pm \rightarrow \pi^0 e^\pm \nu$	$(0.05 \pm 0.03)\%$	$(0.28 \pm 0.14)\%$	$(0.09 \pm 0.05)\%$	$(0.37 \pm 0.17)\%$
$K^\pm \rightarrow \pi^\pm \pi^0$	$(0.05 \pm 0.03)\%$	$(0.18 \pm 0.09)\%$	$(0.06 \pm 0.03)\%$	$(0.18 \pm 0.09)\%$
Opposite sign $K$	–	$(0.04 \pm 0.01)\%$	–	$(0.25 \pm 0.03)\%$
Total background	$(8.65 \pm 0.25)\%$	$(11.62 \pm 0.33)\%$	$(12.08 \pm 0.29)\%$	$(17.67 \pm 0.39)\%$
$K_{\mu 2}$ candidates / $10^6$	18.027	18.433	3.069	3.288
Muon halo	0.39%	0.44%	0.77%	1.22%

tion probability  $P_{\mu e}$  based on a samples of muons from  $K_{\mu 2}$  decays traversing the lead bar collected simultaneously with the  $K_{\mu 2}^\pm(\text{Pb})$  data samples. This sample is electron-free for all practical purposes. The measured probability has been also corrected for the ionization energy loss and bremsstrahlung of muons passing through the lead. A dedicated Geant4 [13] simulation allowed the evaluation of this momentum-dependent correction. The corrected value of  $P_{\mu e}$  provides a measurement of the muon misidentification probability for muon not traversing the lead bar. The correspondent measured background relative to the  $K_{e2}$  sample, integrated over the different samples, is  $(5.64 \pm 0.20)\%$ . The uncertainty comes from the statistics of the  $K_{\mu 2}$  samples traversing the lead bar and from the accuracy in the determination of the correction factors with simulation. Figure 3 shows the uncorrected probability (left) and the correction factors (right).

### 5.2 Beam Halo Background in the $K_{e2}$ Sample

Accidental muons coming from the region upstream to the decay volume mimic the signal in case of  $\mu \rightarrow e \nu_e \nu_\mu$  decay. This background has been measured on data by reconstructing the  $K_{e2}^+$  ( $K_{e2}^-$ ) decay candidates from control samples of positive (negative) tracks collected with the positive (negative) beam blocked. The background is ten times larger in the  $K^-$  sample and comes mainly from the entrance of the decay volume with a strong left-right asymmetry. The analysis exploited those characteristics to minimize this background. The measured contribution integrated over the different samples is  $2.11 \pm 0.09\%$ .

### 5.3 $K^\pm \rightarrow e^\pm \nu \gamma$ background in the $K_{e2}$ sample

The definition of  $R_K$  includes IB, but excludes structure-dependent (SD) radiation. The SD<sup>+</sup> component of the  $K^\pm \rightarrow e^\pm \nu \gamma$  process is kinematically similar to  $K_{e2}$  decay. It mimics the signal if the photon escapes the acceptance of the LKr. The background has been estimated using a MC simulation based on the measured differential decay rate [14]. The background is enhanced in those

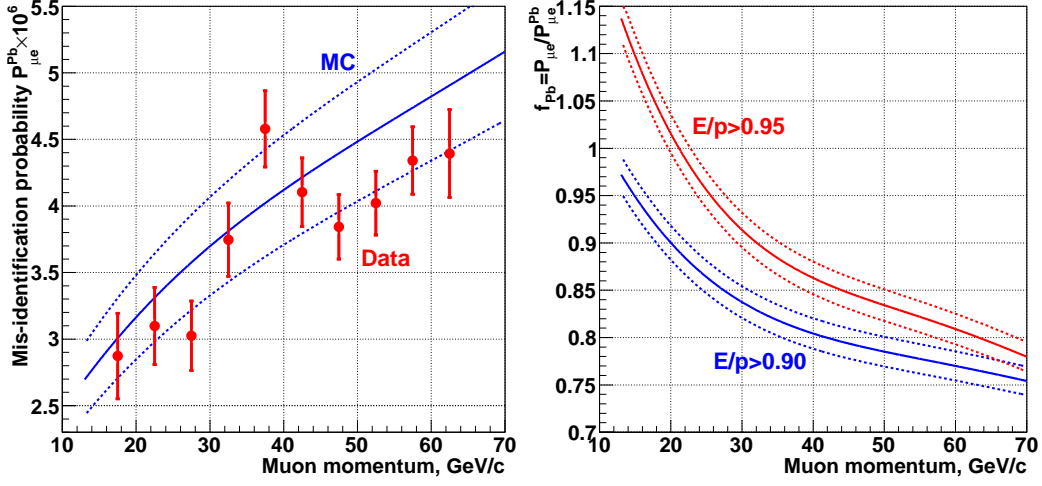


**Figure 3:** (left) Misidentification probability for muons traversing the lead bar,  $P_{\mu e}^{\text{Pb}}$ , for  $(E/p)_{\text{min}} = 0.95$  as a function of momentum: measurement (solid circles with error bars; the uncertainties are uncorrelated) and simulation (solid line). (right) Correction factors  $f_{\text{Pb}} = P_{\mu e} / P_{\mu e}^{\text{Pb}}$  evaluated by a simulation for the two specified values of  $(E/p)_{\text{min}}$ . Dotted lines in both plots indicate the estimated systematic uncertainties arising from the simulation. The correlation of the latter uncertainties across the momentum values leads to a consistent shift of the MC band with respect to the measurements; the data/MC agreement validates the assigned systematic uncertainties.

samples with the lead bar because of the reduced LKr acceptance. The contribution integrated over the different samples is  $2.60 \pm 0.11\%$ . The uncertainty comes from the experimental precision on the measurement of the decay rate.

## 6. Results

The geometrical part of the signal acceptances have been estimated by a MC simulation. The electron and positron identification inefficiency averaged over the  $K_{e2}$  sample is  $(0.72 \pm 0.05)\%$ . It has been measured on data using a sample of  $K^{\pm} \rightarrow \pi^0 e^{\pm} \nu$  and  $K_L \rightarrow \pi^{\pm} e^{\mp} \nu$ .

The  $R_K$  value is obtained through a  $\chi^2$  fit to the measurements in the lepton momentum bins and data taking periods ( $\chi^2/ndf = 47/39$ ). The result is:

$$R_K = (2.488 \pm 0.007_{\text{stat}} \pm 0.007_{\text{syst}}) \times 10^{-5} = (2.488 \pm 0.010) \times 10^{-5}. \quad (6.1)$$

The result is stable within the errors versus lepton momentum and for the independent data samples. A breakdown of the systematic uncertainties is shown in table 2. The main contribution comes from the evaluation of the backgrounds.

The result is consistent with the SM expectation and the achieved precision dominates the world average.

## 7. Conclusions

The most precise measurement of  $R_K$  to date has been performed from a sample of about

**Table 2:** Summary of the uncertainties on  $R_K$ .

Source	$\delta R_K \times 10^5$
Statistical	0.007
$K_{\mu 2}$ background	0.004
$K^\pm \rightarrow e^\pm \nu \gamma$ ( $SD^+$ ) background	0.002
$K^\pm \rightarrow \pi^0 e^\pm \nu$ , $K^\pm \rightarrow \pi^\pm \pi^0$ backgrounds	0.003
Muon halo background	0.002
Spectrometer material composition	0.002
Acceptance correction	0.002
Spectrometer alignment	0.001
Electron identification inefficiency	0.001
1-track trigger inefficiency	0.001
LKr readout inefficiency	0.001
Total systematic	0.007
Total	0.010

$150 \times 10^3$  candidates collected by the NA62 experiment. The result is  $R_K = (2.488 \pm 0.010) \times 10^{-5}$ , consistent with the earlier measurements and with the SM expectation. The experimental uncertainty on  $R_K$  is still an order of magnitude larger than the uncertainty on the SM prediction.

## References

- [1] V. Cirigliano and I. Rosell, Phys. Rev. Lett. **99** (2007) 231801.
- [2] A. Masiero, P. Paradisi and R. Petronzio, Phys. Rev. D **74** (2006) 011701.
- [3] A. Masiero, P. Paradisi and R. Petronzio, JHEP **0811** (2008) 042.
- [4] J. Girrbach and U. Nierste, arXiv:1202.4906 (2012).
- [5] H. Lacker and A. Menzel, JHEP **1007** (2010) 006.
- [6] A. Abada *et al.*, arXiv:1211.3052.
- [7] F. Ambrosino *et al.* [KLOE Collaboration], Eur. Phys. J. C **64** (2009) 627, [Erratum-ibid. **65** (2010) 703].
- [8] C. Lazzeroni *et al.* [NA62 Collaboration], Phys. Lett. B **698** (2011) 105.
- [9] J. Beringer *et al.* (Particle Data Group), Phys. Rev. D **86**, 010001 (2012).
- [10] C. Lazzeroni *et al.* [NA62 Collaboration], Phys. Lett. B **719** (2013) 326.
- [11] J. R. Batley *et al.* [NA48/2 Collaboration], Eur. Phys. J. C **52** (2007) 875.
- [12] V. Fanti *et al.* [NA48 Collaboration], Nucl. Instrum. Meth. A **574** (2007) 433.
- [13] S. Agostinelli *et al.* [GEANT4 Collaboration], Nucl. Instrum. Meth. A **506** (2003) 250.
- [14] F. Ambrosino *et al.* [KLOE Collaboration], Eur. Phys. J. C **64** (2009) 627.